CONSTRAINTS ON STERILE NEUTRINO DARK MATTER CANDIDATE MASS BY THE FERMI GAMMA-RAY BURST MONITOR

ROBERT PREECE
Space Science Department, The University of Alabama in Huntsville, 320 Sparkman Dr., Huntsville AL 35809 USA

KENNY C. Y. NG
Center for Cosmology and AstroParticle Physics (CCAPP), Ohio State University, Columbus, OH 43210 USA

SHUNSAKU HORIUCHI
Center for Neutrino Physics, Department of Physics, Virginia Tech, Blacksburg, VA 24061 USA

JENNIFER GASKINS
GRAPPA, University of Amsterdam, 1098 XH Amsterdam, Netherlands

MILES SMITH
Pennsylvania State University, PA 16802 USA

The Fermi Gamma-Ray Burst Monitor (GBM) is an all-sky gamma-ray detector operating in low-earth orbit since 2008. The 12 individual NaI scintillation detectors have a roughly cosine angular response, which limits the ability to detect point sources to an accuracy of several degrees radius. Still, a diffuse source at the Galactic Center should be detectable. Assuming a sterile neutrino Dark Matter candidate that decays to an active neutrino and a photon, we present search results for a line signal from the Galactic Center in the hard X-ray regime.

1 Motivation

The Gamma-ray Burst Monitor (GBM), on board the *Fermi* Gamma-ray Space Telescope mission, views the entire unocculted sky in the energies between 8 keV and 40 MeV. The lower energies (below 1 MeV) are observed by 12 Sodium Iodide (NaI) detectors that have modest localization capabilities. The primary science objectives of GBM are the detection and analysis of gamma-ray bursts. However, the instrument's versatility allows the study of other transient sources, such as solar flares, soft gamma-ray repeaters and terrestrial gamma flashes, as well as the continuous monitoring of soft gamma-ray sources in the Galaxy and pulsar timing analyses. We present here an effort to use GBM observations of the Galactic Center as an indirect search for sterile neutrinos as a dark matter candidate.

Massive sterile neutrinos can radiatively decay to active neutrinos, producing a photon line signal at half the sterile neutrino mass [1,2,3]. Meanwhile, sterile neutrinos produced by neutrino oscillations in the early universe can satisfy the abundance constraints for being a dark matter (DM) candidate, if they have a mass on the order of 1–100 keV range [4,5,6]. X-ray telescopes have already been searching for spectral lines from keV neutrinos [7,8,9] and (model-dependent) constraints have been obtained from Lyman alpha measurements (probing clustering in the early universe) [10]. However, a window of parameter space remains between 12 and 40 keV, while with

a low-energy cutoff of 8 keV, GBM can put constraints on line emission at half the mass above 16 keV.

2 The Fermi Gamma-Ray Burst Monitor

The GBM was designed to support the Large Area Telescope (LAT) on *Fermi*, which nominally observes in a sky survey mode, resulting in the spacecraft pointing typically within 50° of zenith. GBM NaI detectors 0 and 6 point within $\sim 20°$ of the LAT pointing direction, however, the spacecraft blocks part of their field of view [11]. For this analysis, we use detector 7, which has good sky coverage (also close to the LAT pointing direction) but has minimal problems with spacecraft blockage. NaI 7 is also not on the Sun-facing side of the spacecraft, so it suffers relatively little soft X-ray contamination from the Sun.

The NaI detectors do not record the arrival direction of each photon; rather, the effective area defines the relevant field of view (FOV). The flat geometry of the NaI crystals, plus attenuation by the housing materials, result in an angular response very similar to the cosine of the detector zenith angle. At low energies, the effective area is close to 0 at incidence angles $\geq 90°$, but note that the response is non-negligible over half the sky. As a function of energy, the effective area increases rapidly from the threshold of 8 keV up to ~ 30 keV. Thus, assuming a line signal from a distribution of DM concentrated at the Galactic Center, it doesn't matter how the DM is distributed, most of it will be contained within 60°, corresponding to the GBM FOV.

2.1 Arrival direction analysis tools for GBM

Since it is not possible to correctly calculate a flux within a limited region-of-interest (ROI), due to lack of individual photon tracking and extremely broad "FOV" of the GBM detectors, we created a suite of tools for directional analysis of GBM data. This includes a tool to calculate the count rate in a specified NaI detector as a function of Galactic pointing direction, based on the actual pointing and livetime history of *Fermi*, which uses public data files (GBM CSPEC files and LAT FT2 files). This is discussed in section 2.2 below. We have also developed a tool to simulate NaI counts data from an input source model, which accounts for the NaI effective area as a function of inclination angle and photon energy. Using this tool, the count rate in a specified NaI detector as a function of Galactic pointing direction can be predicted for a theoretical model.

2.2 The X-ray sky as seen by GBM

Figure 1 is an example of GBM count rate maps as a function of the detector pointing direction of NaI detector 7 in Galactic coordinates for three different energies: 10-11 keV, 16-17 keV and 40-42 keV. Note that this is *not* a flux map, which would require knowledge of the arrival direction of each count. The map is constructed by first dividing the sky into 768 equal-area pixels (using HEALPix[a]) and then using the LAT FT2 files to determine the detector zenith pointings that correspond with each pixel. The GBM data set is filtered, excluding data time intervals containing GRBs and other transients, passages through the South Atlantic Anomaly (where the instrument is turned off) and high magnetic latitude regions (to avoid elevated charged particle rates). We also eliminate times when the Earth may be in the field of view. The remaining count rates are then averaged for each sky pixel. The result is a map of the count rates seen by the detector, averaged over the effective area angular response.

Soft X-ray sources centered on the Galactic Center (GC) are clearly detected by this technique, as seen in the top left panel in Figure 1. As expected, no features are significant, due

[a] http://healpix.jpl.nasa.gov [12]

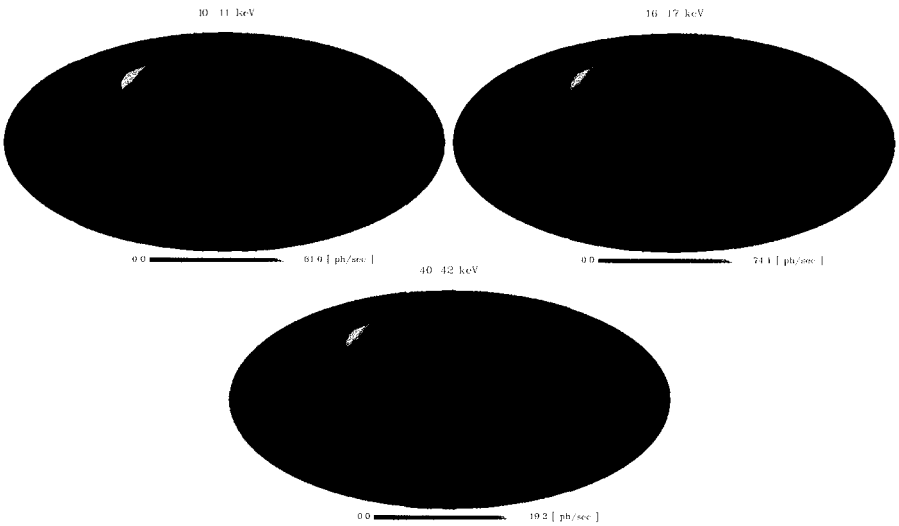

Figure 1 – The final counts rate sample from 4 years of data from NaI detector 7, which corresponds to 4.6 million seconds ($\sim$ 53 days) of live time after data cuts. The pixel position corresponds to the pointing direction of the detector normal. The grey pixels are where no observing time is registered after the selection cuts.

to the blurring by the angular response. At higher energies, instrumental backgrounds dominate over astrophysical signals, so the enhancement of count rates at the GC fades into the background.

The counts spectrum (not shown) for the final data sample for both GC ROI ($\psi < 60°$) and anti-GC ROI ($\psi > 120°$) chosen to have the same solid angle, has as its dominant component a power-law plus various background lines. There is an additional excess at low energies towards the GC region that suggests the rise of the astrophysical component.

3 Sterile Neutrino Line Strength Analyses

Two analyses are presented in Figure 2. For the first, we require that the flux from a dark matter signal doesn't exceed the total measured count rate in the energy bin of the line, in the selected ROI. This 'total flux' constraint is quite robust and conservative. For the second analysis, we choose a window around each line energy (larger than expected line signal width) and model the spectrum as a line signal (at fixed energy) plus a power law. The fitted line intensity is the smallest signal to yield a worse fit than the background only hypothesis at the 95% level and thus provides a constraint on the mixing angle between active and sterile neutrinos.

In the mass range shown in Figure 2, the best previous constraints are set by observations of the cosmic X-ray background (CXB) by HEAO-1 [13], the Milky Way (MW) halo from INTEGRAL [14], as well as a model-dependent lower bound based upon DM abundance [15].We show the new limits derived in this work, one derived only from the total flux, and the other derived using spectral line fitting. The spectral analysis is stronger than that from prior studies by about an order of magnitude.

Acknowledgments

We thank Mark Finger (Universities Space Research Association, Huntsville) for providing transient cuts for the GBM data. This work is supported by NASA grant NNX11AO46G. K.C.Y.N.

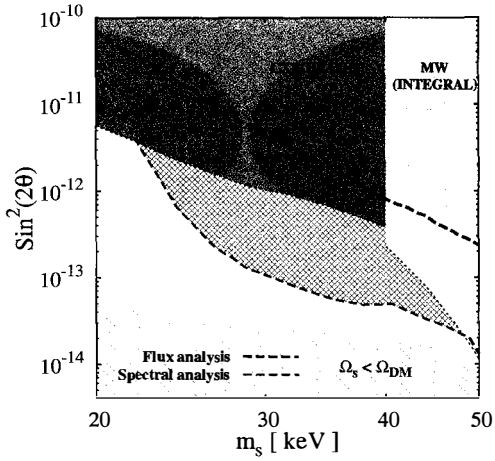

Figure 2 – Constraints from X-ray missions on sterile neutrino dark matter decays, which depends on the mixing angle, $\sin^2(2\theta)$, and the mass, m_s.

was supported by NSF Grants PHY-1101216 and PHY-1404311. J.G. acknowledges support from NASA through Einstein Postdoctoral Fellowship grant PF1-120089 awarded by the Chandra X-ray Center, which is operated by the Smithsonian Astrophysical Observatory for NASA under contract NAS8-03060.

References

1. P. B. Pal and L. Wolfenstein, Phys. Rev. D **25**, 766 (1982).
2. V. D. Barger, R. Phillips, and S. Sarkar, Phys. Lett. B **352**, 365 (1995), hep-ph/9503295.
3. K. Abazajian, G. M. Fuller, and W. H. Tucker, Astrophys. J. **562**, 593 (2001), astro-ph/0106002.
4. S. Dodelson and L. M. Widrow, Phys. Rev. Lett. **72**, 17 (1994), hep-ph/9303287.
5. X.-D. Shi and G. M. Fuller, Phys. Rev. Lett. **82**, 2832 (1999), astro-ph/9810076.
6. K. Abazajian, G. M. Fuller, and M. Patel, Phys. Rev. D **64**, 023501 (2001), astro-ph/0101524.
7. H. Yuksel, J. F. Beacom, and C. R. Watson, Phys. Rev. Lett. **101**, 121301 (2008), 0706.4084.
8. A. Boyarsky, O. Ruchayskiy, and M. Markevitch, Astrophys. J. **673**, 752 (2008), astro-ph/0611168.
9. M. Loewenstein, A. Kusenko, and P. L. Biermann, Astrophys. J. **700**, 426 (2009), 0812.2710.
10. Seljak, U., Slosar, A., & McDonald, P., J. Cosmol. Astropart. P. **10**, 014 (2006)
11. C. Meegan *et al.*, Astrophys. J. **702**, 791 (2009), 0908.0450.
12. K. Gorski *et al.*, Astrophys. J. **622**, 759 (2005), astro-ph/0409513.
13. A. Boyarsky, A. Neronov, O. Ruchayskiy, M. Shaposhnikov, and I. Tkachev, Phys. Rev. Lett. **97**, 261302 (2006), astro-ph/0603660.
14. A. Boyarsky, D. Malyshev, A. Neronov, and O. Ruchayskiy, MNRAS **387**, 1345 (2008), 0710.4922.
15. A. Boyarsky, O. Ruchayskiy, and M. Shaposhnikov, Ann. Rev. Nucl. Part. Sci. **59**, 191 (2009), 0901.0011.